Proceedings of the 8th International Symposium on Mathematical Morphology,
Rio de Janeiro, Brazil, Oct. 10–13, 2007, MCT/INPE, v. 1, p. 101–112.
http://urlib.net/dpi.inpe.br/ismm@80/2007/03.19.15.04

A scale-space toggle operator for morphological segmentation

Leyza B. Dorini and Neucimar J. Leite

Instituto de Computação (IC), Universidade Estadual de Campinas (Unicamp), SP, Brazil
{ldorini,neucimar}@ic.unicamp.br

Abstract The analysis of different representation levels has been largely used to handle the multiscale nature of image data. Here, we explore the scale-space properties of a toggle operator defined on a scaled morphological framework. These properties conduce to a well-controlled image extrema simplification, yielding sound segmentation and filtering results even when the operator is used in a binarization process. Also, the watershed transform using markers extracted from the processed image gives better segmentation results than when using markers from the original one. To show the robustness of our approach, we carried out tests on images of different classes and subjected to different lighting conditions.

Keywords: scale-space, scale-dependent morphology, image segmentation.

1. Introduction

Multiscale approaches have been largely considered in several signal processing applications, allowing the analysis of different representation levels and, further, the choice of the ones exhibiting the interest features.

One of the basic problems that arises when using multiscale methods originates from the difficulty to relate meaningful information of the signal across scales. In [20], Witkin proposed a novel multiscale approach, named scale-space, where the representation of an interest signal feature describes a continuous path through the scales. In such a way, it is possible to relate information obtained in different representation levels, as well as to have a precise localization of the interest features in the original signal.

Another important characteristic is that the transformation to a coarser level in the scale-space representation does not introduce artifacts, that is, signal features present at a scale σ are also present at all finer scales. This property is called monotonicity, since the number of features must necessarily be a monotonic decreasing function of scale [20].

Since the introduction of the scale-space theory, a large number of formulations have been proposed, based on different assumptions. In the linear approach, formalized by Witkin [20], a family of images is generated by convolving the original image with a Gaussian kernel. The signal extrema and

Proceedings of the 8th International Symposium on Mathematical Morphology,
Rio de Janeiro, Brazil, Oct. 10–13, 2007, MCT/INPE, v. 1, p. 101–112.
http://urlib.net/dpi.inpe.br/ismm@80/2007/03.19.15.04

its first derivative constitute the features of interest. However, any convolution kernel used to obtain the scale-space introduces new extrema (the image maxima and minima) as the scale increases and, thus, the monotonicity property for linear filters and signal extrema does not hold [9]. To avoid this problem, other linear and non-linear approaches have been introduced [2].

Here, we explore the scale-space properties of a toggle-based operator in segmentation applications. The operator is defined in a scaled morphological framework using concave structuring functions, which was proved to have contrast properties [14]. Furthermore, it considers local pixel information (not only scale knowledge) to determine if each pixel should be processed by erosion or dilation, in contrast to other multiscale approaches that take into account mainly global information. All this characteristics conduce to an image simplification that enables the identification of important image structures using very simple operations, even in ill-illuminated images.

The next section presents basic multiscale morphology definitions. Section 3 defines the scale-space toggle operator and some of its main properties. Finally, we show some results in Section 4 and draw some conclusions and future work perspectives in Section 5.

2. Morphological-based scale-space

The notion of scale is related to the way we observe the physical world, where different features are made explicit at different scales. In mathematical morphology, the concept of scale (or size) dependent observations was introduced by Matheron [11] in his work on granulometry, which captures the size distribution of spatial observations.

To introduce the notion of scale, we can make the basic morphological operations of erosion and dilation scale-dependent by defining a scaled structuring function $g_\sigma : \mathcal{G}_\sigma \subset \mathbb{R}^2 \to \mathbb{R}$, such that [4]

$$g_\sigma(\mathbf{x}) = |\sigma| g(|\sigma|^{-1}\mathbf{x}) \quad \mathbf{x} \in \mathcal{G}_\sigma, \forall \sigma \neq 0, \tag{1}$$

where $\mathcal{G}_\sigma = \{\mathbf{x} : \|\mathbf{x}\| < \mathcal{R}\}$ is the support region of the function g_σ. To ensure reasonable scaling behavior, some other conditions are necessary [4], requiring a monotonic decreasing structuring function along any radial direction from the origin. In this paper, we use as structuring function $g(x, y) = -\max\{x^2, y^2\}$, that in the scaled version is given by

$$g_\sigma(x, y) = -|\sigma|^{-1} \max\{x^2, y^2\}, \tag{2}$$

where σ represents the scale. Observe that, for a 3×3 structuring element (used in this work), g_σ is zero at position $\mathbf{0}$ and $-|\sigma|^{-1}$ otherwise. Figure 1 illustrates the structuring function.

Scaled morphological operators have been frequently associated to non-linear filters and scale-space theory. Jackway [4] introduced a scale-space

Proceedings of the 8th International Symposium on Mathematical Morphology,
Rio de Janeiro, Brazil, Oct. 10–13, 2007, MCT/INPE, v. 1, p. 101–112.
http://urlib.net/dpi.inpe.br/ismm@80/2007/03.19.15.04

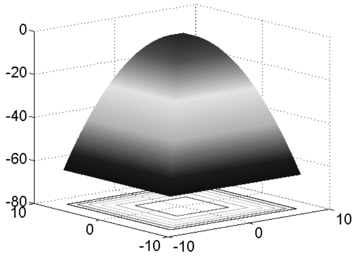

Figure 1. The structuring function.

based on the Multiscale Morphological Dilation Erosion (MMDE) operator, which unifies the scaled erosion and dilation transformations so that both positive and negative scales are taken into account (the image is processed by dilation, for positive scales, and by erosion for the negative ones). The interest features are the watershed of the smoothed signal in a certain scale. However, this method cannot be directly associated with image segmentation since "the watershed arcs moves spatially with varying scale" [3, 4].

In [7, 8], Leite and Teixeira explored the extrema preservation property of MMDE by using the extrema set obtained during the filtering process as markers in a homotopic modification of the original image, avoiding the spatial shifting of the watershed lines. They controlled the extrema merging through the different scales, obtaining good segmentation results. The authors also defined a new operator that explores the idempotence of the MMDE, establishing a relation between the structuring function g_σ and the extremes that persist at a given scale σ.

Scaled morphological operators have also been applied for image sharpening. Kramer [5] proposed a non-linear operator that replaces the original gray value of a pixel by the local minimum or maximum, depending on what value is closer to the original one. Shavemaker et al. [14] generalized this result by defining a new class of iterative scaled morphological image operators. In fact, they proved that all the operators that use a concave structuring function have interesting sharpening properties. Here, we explore some important characteristics of these operators to introduce a toggle transformation having interesting scale-space extrema preservation properties, as explained next.

3. Operator definition

A toggle operator has two major points: the primitives and a given decision rule [16]. Here, we use as primitives an extensive and an anti-extensive transformation, namely, the scale dependent dilation and erosion. The decision rule involves, at a point $\mathbf{x}$, the value $f(\mathbf{x})$ and the primitives results.

Proceedings of the 8th International Symposium on Mathematical Morphology,
Rio de Janeiro, Brazil, Oct. 10–13, 2007, MCT/INPE, v. 1, p. 101–112.
http://urlib.net/dpi.inpe.br/ismm@80/2007/03.19.15.04

Formally:

$$(f \oslash g_\sigma)^k(\mathbf{x}) = \begin{cases} \psi_1^k(\mathbf{x}) & \text{if } \psi_1^k(\mathbf{x}) - f(\mathbf{x}) < f(\mathbf{x}) - \psi_2^k(\mathbf{x}), \\ f(\mathbf{x}) & \text{if } \psi_1^k(\mathbf{x}) - f(\mathbf{x}) = f(\mathbf{x}) - \psi_2^k(\mathbf{x}), \\ \psi_2^k(\mathbf{x}) & \text{otherwise,} \end{cases} \tag{3}$$

where $\psi_1^k = (f \oplus g_\sigma)^k$, that is, the dilation of f with the scaled structuring function g_σ, k times. In the same way, $\psi_2^k = (f \ominus g_\sigma)^k$.

In the following, we analyze the operator's behavior regarding on scale changing and on the recursive application of the primitives.

3.1 Changing the number of iterations

To avoid undesirable effects such as halos and oscillations, idempotent toggle operators are used [15]. Since the defined operator (Equation 3) is not idempotent, we use an alternative solution to this problem based on the specific knowledge of the pixels transformation. The following proposition formalizes an important property of the operator (see proof in [6]), which guarantees that it has a well-controlled behavior.

Proposition 1. *Let $\boldsymbol{x}$ be a pixel of the image and g be a structuring function with a single maximum at the origin, that is, $g(\boldsymbol{x})$ is a local maximum implies $\boldsymbol{x} = \boldsymbol{0}$. The sequence defined by $(f \oslash g_\sigma)^k(\boldsymbol{x})$ is stationary and monotonic increasing (decreasing) until a certain iteration k_0, while it is monotonic decreasing (increasing) after the iteration k_0.*

This property states that a pixel can initially converge to a specific local minimum and, after a certain iteration, to converge to an image maximum, or vice-versa [6]. Furthermore, since the sequence is stationary, we have the guarantee that it converges to a constant value, that is, it stabilizes after a certain number of iterations. Note that k_0 can be 1, that is, a pixel transformed value is strictly increasing or decreasing.

In Figure 2, as the number of iterations increases, the influence zone of the deeper minimum m_2 grows significantly, in such a way that the value of $f(m_1)$ become closer to the dilated values, and stabilizes after 10 iterations.

At this step, we can conclude that, in some neighborhood of an important minimum (maximum), the pixels values will be eroded (dilated) in such a way that it is possible to identify the significant extrema of the image and their influence zones. In this sense, we can define a new thresholding operation that uses a decision rule similar of that in Equation 3:

$$(f \oslash g_\sigma)^k(\mathbf{x}) = \begin{cases} 255 & \text{if } \psi_1^k(\mathbf{x}) - f(\mathbf{x}) <= f(\mathbf{x}) - \psi_2^k(\mathbf{x}) \\ 0 & \text{otherwise,} \end{cases} \tag{4}$$

where, again, $\psi_1^k(\mathbf{x}) = (f \oplus g_\sigma)^k(\mathbf{x})$, that is, the dilation of $f(\mathbf{x})$ with the scaled structuring function g_σ k times. In the same way, $\psi_2^k(\mathbf{x}) =$

Proceedings of the 8th International Symposium on Mathematical Morphology,
Rio de Janeiro, Brazil, Oct. 10–13, 2007, MCT/INPE, v. 1, p. 101–112.
http://urlib.net/dpi.inpe.br/ismm@80/2007/03.19.15.04

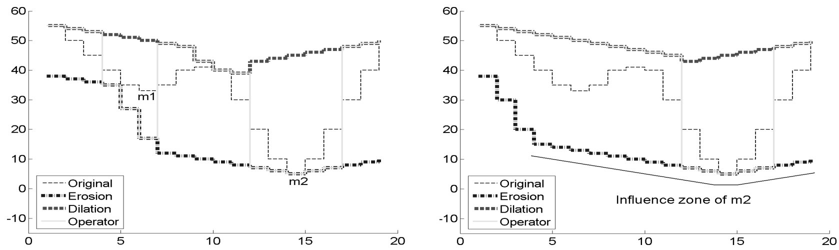

(a) After seven iterations (b) After ten iterations

Figure 2. Operator behavior through different iterations using $g = [-1\ 0\ \ -1]$.

$(f \ominus g_\sigma)^k(\mathbf{x})$. This binary approach yields sound segmentation and filtering results, as we shall illustrate in Section 4.1.

3.2 Changing the scale

By taking into account the increasing of scale, the defined transformation (Equation 3) results in a new scale-space definition. The following proposition states that if an extrema of the signal is present at a given scale σ, it must be found at all the intermediate scales.

Proposition 2 (Behaviour of image extrema)**.** *Let g be a structuring function with a single maximum at the origin, that is, $g(\boldsymbol{x})$ is a local maximum implies $\boldsymbol{x} = \boldsymbol{0}$. To avoid level-shifting and horizontal translation effects, we require that $\sup_{t \in \mathcal{G}}\{g(\boldsymbol{t})\} = 0$, and $g(\boldsymbol{0}) = 0$. Thus*

1. *if $(f \oslash g_\sigma)(\boldsymbol{x}_{max})$ is a local maximum, then $f(\boldsymbol{x}_{max})$ is a local maximum of $f(\boldsymbol{x})$ and $(f \oslash g)(\boldsymbol{x}_{max}) = (f \oplus g)(\boldsymbol{x}_{max}) = f(\boldsymbol{x}_{max})$,*

2. *if $(f \oslash g_\sigma)(\boldsymbol{x}_{min})$ is a local minimum, then $f(\boldsymbol{x}_{min})$ is a local minimum of $f(\boldsymbol{x})$ and $(f \oslash g)(\boldsymbol{x}_{min}) = (f \ominus g)(\boldsymbol{x}_{max}) = f(\boldsymbol{x}_{min})$,*

3. *If $0 < \sigma_1 < \sigma_2$ and $(f \oslash g_{\sigma_2})(\boldsymbol{x}_{max})$ is a local maximum, then $(f \oslash g_{\sigma_1})(\boldsymbol{x}_{max})$ is a local maximum and $(f \oslash g_{\sigma_1})(\boldsymbol{x}_{max}) = (f \oslash g_{\sigma_2})(\boldsymbol{x}_{max})$,*

4. *If $0 < \sigma_1 < \sigma_2$ and $(f \oslash g_{\sigma_2})(\boldsymbol{x}_{min})$ is a local minimum, then $(f \oslash g_{\sigma_1})(\boldsymbol{x}_{min})$ is a local minimum and $(f \oslash g_{\sigma_1})(\boldsymbol{x}_{min}) = (f \oslash g_{\sigma_2})(\boldsymbol{x}_{min})$.*

These results (see proofs in Appendix) guarantee that the number of extrema does not decrease when the scale tends to zero. This aspect constitutes the morphological scale-space monotonicity property.

Theorem 1 (Monotonicity Theorem)**.** *Monotonicity property for the defined scale-space. Let $f : \mathcal{D}_f \subseteq \mathbb{R}^n \to \mathbb{R}$ be a limited function, $g_\sigma : \mathcal{G}_\sigma \subseteq \mathbb{R}^n \to \mathbb{R}$ be a structuring function that satisfies the properties of Proposition 1, and the following set of points $E_{max}(f) = \{\boldsymbol{x} : f(\boldsymbol{x})$ is a local*

Proceedings of the 8th International Symposium on Mathematical Morphology,
Rio de Janeiro, Brazil, Oct. 10–13, 2007, MCT/INPE, v. 1, p. 101–112.
http://urlib.net/dpi.inpe.br/ismm@80/2007/03.19.15.04

maximum} and $E_{min}(f) = \{\boldsymbol{x} : f(\boldsymbol{x})$ *is a local minimum}* *represent the extrema points of* f. *Then, for any* $0 < \sigma_1 < \sigma_2$,

$$E_{min}(f \oslash g_{\sigma_2}) \subseteq E_{min}(f \oslash g_{\sigma_1}) \subseteq E_{min}(f), \text{ and}$$
$$E_{max}(f \oslash g_{\sigma_2}) \subseteq E_{max}(f \oslash g_{\sigma_1}) \subseteq E_{max}(f).$$

That is, the number of local maxima (minima) decreases monotonically with the increase of scale [4].

Finally, proposition 3 states that the operator approaches $f(x)$ as the scale parameter approaches zero. In other words, as $\sigma \to 0$, the value of the operator converges to the original image value (see proof in Appendix).

Proposition 3 (Convergence to the original image value)**.** *If the signal* $f(\boldsymbol{x}) : \mathcal{D}_f \subseteq \mathbb{R}^n \to \mathbb{R}$ *is continuous at some* $\boldsymbol{x} \in \mathcal{D}_f$, *then* $(f \oslash g_\sigma)(\boldsymbol{x}) \to f(\boldsymbol{x})$ *as* $\sigma \to 0$.

4. Results

First, we give some examples of the binary transformation represented by Equation 4, where segmentation and filtering results are easily obtained. After, we apply the h-maxima transform in the image processed by Equation 3, to further extract markers to be used in a watershed transform.

4.1 Binary results

The first example shows the segmentation of a historical document in which the front side of the paper contains ink components from its verso side. The results were compared against the moving averages [19] algorithm, specially designed for segmenting text images. This method considers a threshold based on the mean gray level of the last n pixels. Figure 3 illustrates the better performance of our operator in the sense that it suppresses properly the components belonging to the reverse side of the paper.

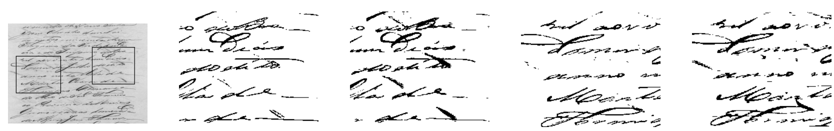

(a) (b) (c) (d) (e)

Figure 3. Segmentation example for a historical document image. (a) Original image, and segmentation results for two select regions using the moving averages algorithm ((c) and (e)) and the proposed operator ((b) and (d)).

The second experiment was carried out based on a set of images with varying lighting conditions (linear, Gaussian and sine-wave) [13], and on a

Proceedings of the 8th International Symposium on Mathematical Morphology,
Rio de Janeiro, Brazil, Oct. 10–13, 2007, MCT/INPE, v. 1, p. 101–112.
http://urlib.net/dpi.inpe.br/ismm@80/2007/03.19.15.04

set of well-known threshold-based segmentation methods described in literature, namely, moving averages [19], regional thresholds [13], and the Otsu's [12] thresholding algorithm. An evaluation of these methods as well as the set of considered images can be found in [13]. Figure 4 shows the segmentation results for the mentioned algorithms and for the operator defined by Equation 4.

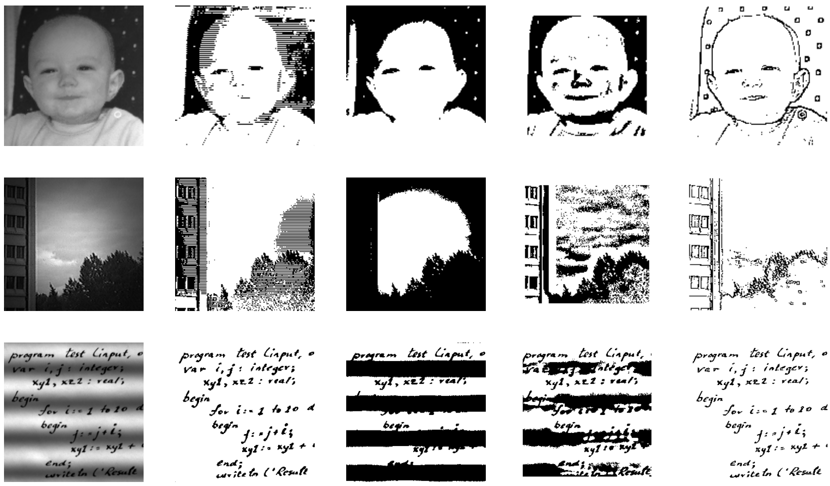

(a) (b) (c) (d) (e)

Figure 4. Segmentation results for images with different illumination conditions (linear, Gaussian and sine-wave, respectively). (a) original image, (b) moving averages, (c) Otsu's method, (d) regional thresholding and (e) proposed operator ((i) facel (for $k = 1$ and $\sigma = 0.1$), (ii) skyg (for $k = 1$ and $\sigma = 0.06$) and (iii) pascals (for $k = 2$ and $\sigma = 0.1$).

This well-controlled behavior reflects the results of the previous propositions. The image extrema merge in an organized way, and no new maxima or minima are created, according to the morphological scale-space theory which constitutes the basis of our approach. Finally, note that the operator selects one threshold per pixel based on local features, as it is the case for dynamic thresholdings.

4.2 Gray-scale results

Image segmentation consists basically on partitioning an image into a set of disjoint (non-overlapping) and homogeneous regions which are supposed to correspond to image objects that are meaningful to a certain application. In a morphological framework, this is typically done by first extracting markers of the significant structures, and then using the watershed transform [1] to extract the contours of these structures as accurately as possible.

Proceedings of the 8th International Symposium on Mathematical Morphology,
Rio de Janeiro, Brazil, Oct. 10–13, 2007, MCT/INPE, v. 1, p. 101–112.
http://urlib.net/dpi.inpe.br/ismm@80/2007/03.19.15.04

Although image extrema are frequently used as markers, they can also correspond to insignificant structures or noise. Thus, to prevent the over-segmentation problem, it is necessary to select image extrema according to some criteria, such as contrast, regions area and so forth. A typical approach consists on use the h-maxima (h-minima) transform to suppress all image maxima (minima) whose contrast is lower than a specified value h, and use the extended (regional) extrema as markers.

This notion is closely related to the concept of dynamics, that assigns to each image extrema a value that characterizes the persistence of the structure it marks when applying increasing contrast filters (in other words, the minimal size of the contrast filter for which the extrema is eliminated). Indeed, a regional extrema of an image f is also an extrema of its h-maxima transform only if the structure it marks has contrast higher than h, which also implies a dynamics higher than h [17, 18].

In this paper, we apply the h-maxima transform to select the image maxima that should be used as markers in a watershed transform. The methodology is summarized in the Algorithm 1 below.

Algorithm 1 Segmentation procedure using h-extrema as markers.

1: given a height h and an input image I;
2: generate a transformed image, $I1$, applying Eq. 3 on I;
3: compute the *h-maxima* of $I1$;
4: extract the extended (regional) maxima;
5: compute the watershed transform using these maxima as markers.

Quantifying the results of a segmentation algorithm is a challenging task, since this remains a ill-defined problem. Here, we perform a qualitative analysis of the results based on some specific criteria, such as robustness to badly illuminated images. We also compute steps $3-5$ of Algorithm 1 in the original image I, and compare the results against ours.

Figure 5 and Figure 6 show the segmentation results obtained for ill-illuminated images used previously (the parameters are in the Figures' captions). In the last column of each figure, we show the best results obtained using markers from the original image. The markers extracted from the transformed image are less sensitive to illumination problems, yielding a segmentation that enhances the most important structures of the image without introducing artifacts. In Figure 6, we can see that our approach separates correctly the main regions of the figure.

Figure 7 shows the segmentation results, by considering different values of h, for the *road* image transformed by the operator defined in Equation 3 using scale 60 and one iteration. Note that, as the value of h increases, less structures are marked and, thus, less regions are segmented.

Figure 8 shows the segmentation results for the well-known *cameraman* image. As in the previous cases, the quantity of segmented regions depends

Proceedings of the 8th International Symposium on Mathematical Morphology,
Rio de Janeiro, Brazil, Oct. 10–13, 2007, MCT/INPE, v. 1, p. 101–112.
http://urlib.net/dpi.inpe.br/ismm@80/2007/03.19.15.04

(a) (b) (c) (d)

Figure 5. Segmentation results for the *skyg* image. (a) original image, and using transformed images (b) $\sigma = 60$ and $k = 1$, with $h = 2$; (c) $\sigma = 60$ and $k = 1$, with $h = 10$, and (d) based on the original image using $h = 10$.

(a) (b) (c)

Figure 6. Segmentation results for the *facel* image. (a) original image, (b) using transformed image $\sigma = 10$ and $k = 5$, with $h = 45$, and (c) based on the original image using $h = 45$.

(a) (b) (c) (d)

Figure 7. Segmentation results for the *road* image, (a) original image, and using transformed images $\sigma = 60$ and $k = 1$ with (b) $h = 5$, (c) $h = 20$ and (d) $h = 40$.

on the relationship between the σ and h values.

The dynamics' principle can be applied to other families of increasing morphological filters by reconstruction, not only to contrast filters [17]. Figure 9 shows the results obtained for the *lenna* image when including an opening by reconstruction between the steps 3 and 4 of the Algorithm 1. We also make an opening by reconstruction in the original image and further extract the extended maxima to compare the results. Figure 9(b)-(c) show the results for the original image and Figure 9(d)-(e) for the transformed image. In the following, we present some overall conclusions.

Proceedings of the 8th International Symposium on Mathematical Morphology,
Rio de Janeiro, Brazil, Oct. 10–13, 2007, MCT/INPE, v. 1, p. 101–112.
http://urlib.net/dpi.inpe.br/ismm@80/2007/03.19.15.04

(a) (b) (c)

Figure 8. Segmentation results for the *cameraman* image. (a) Original image and using transformed images (b) $\sigma = 15$ and $k = 10$, with $h = 80$ and (c) $\sigma = 31$ and $k = 2$, with $h = 31$.

(a) (b) (c) (d) (e)

Figure 9. Segmentation results for the *lenna* image. (a) original image, using original image with (b) $h = 11$, (c) $h = 21$, and using transformed images (d) $\sigma = 21$ and $k = 2$, with $h = 21$, and (e) $\sigma = 31$ and $k = 2$, with $h = 31$.

5. Conclusions

In this paper, we explored a new scale-space toggle operator, taking into account the strong monotonicity property for regions of a 2D signal, according to the morphological scale-space theory discussed in literature [4, 20]. The defined operator uses concave structuring functions, which was proved to have contrast properties [14].

In our approach, we deal with transformations of the image maxima and minima at the same time. This aspect, together with the monotonicity property, guarantees that we have an extrema merging simplification that considers the relation between the image extrema along the whole transformation.

We work with an explicit notion of scale guided by the scale-space theory, using a toggle transformation for segmentation problems, unlike the other applications of this operator which consider mainly problems related to image contrast enhancement.

Results comprove the robustness of our approach when dealing with ill-illuminated images. Also, the image simplification obtained using Equation 3 allows a more effective marker extraction.

As a future work, we will deal with problems of locally controlling the extrema merging by taking into account the height of the structuring functions and the distance between the image extrema in the definition of a parametric mapping using both these information.

Proceedings of the 8th International Symposium on Mathematical Morphology,
Rio de Janeiro, Brazil, Oct. 10–13, 2007, MCT/INPE, v. 1, p. 101–112.
http://urlib.net/dpi.inpe.br/ismm@80/2007/03.19.15.04

References

[1] S. Beucher and F. Meyer, *The morphological approach to segmentation: the watershed transformation*, Mathematical Morphology in Image Processing (1993), 433–481.

[2] H. J. A. M. Heijmans and R. van den Boomgaard, *Algebraic Framework for Linear and Morphological Scale-Spaces*, Journal of Visual Communication and Image Representation **13** (2002), 269–301.

[3] P. T. Jackway, *Gradient watershed in morphological scale-space*, IEEE Transactions on Image Processing **15** (1996), 913–921.

[4] P. T. Jackway and M. Deriche, *Scale-space properties of the multiscale morphological dilation-erosion*, IEEE Transactions on Pattern Analysis and Machine Intelligence **18** (1996), 38–51.

[5] H. P. Kramer and J. B. Bruckner, *Iterations of a non-linear transformation for enhancement of digital images*, Pattern Recognition **7** (1975), 53–58.

[6] N. J. Leite and L. E. B. Dorini, *A scaled morphological toggle operator for image transformations*, XIX Brazilian Symposium on Computer Graphics and Image Processing, Proceedings..., 2006, pp. 323–330.

[7] N. J. Leite and M. D. Teixeira, *Morphological scale-space theory for segmentation problems*, IEEE-EURASIP Workshop on Nonlinear Signal and Image Processing, 1999, pp. 364–368.

[8] ______, *An idempotent scale-space approach for morphological segmentation*, Mathematical Morphology and its Applications to Image and Signal Processing, 2000, pp. 291–300.

[9] L. M. Lifshitz and S. M. Pizer, *A multiresolution hierarchical approach to image segmentation based on intensity extrema*, IEEE Transactions on Pattern Analysis and Machine Intelligence **12** (1990), no. 4, 529–540.

[10] J. E. Marsden and M. J. Hoffman, *Elementary Classical Analysis*, Freeman, 1993.

[11] G. Matheron, *Random Sets and Integral Geometry*, John Wiley and Sons, 1975.

[12] N. Otsu, *A threshold selection method from grey-level histograms*, IEEE Transactions on Systems, Man and Cybernetics **9** (1979), no. 1, 377–393.

[13] J. R. Parker, *Algorithms for Image Processing and Computer Vision*, Wiley, 1996.

[14] J. G. M. Schavemaker, M. J. T. Reinders, J. J. Gerbrands, and E. Backer, *Image sharpening by morphological filtering*, Pattern Recognition **33** (2000), 997–1012.

[15] J. Serra and L. Vicent, *An overview of morphological filtering*, Circuits, Systems and Signal Processing **11** (1992), no. 1, 47–108.

[16] P. Soille, *Morphological Image Analysis: Principles and Applications*, Springer-Verlag, 2003.

[17] C. Vachier and L. Vicent, *Valuation of image extrema using alternating filters by reconstruction*, SPIE Neural, Morphological, and Stochastic Methods in Image and Signal Processing, 1995, pp. 94–103.

[18] C. Vachier and F. Meyer, *Extinction value: a new measurement of persistence*, IEEE Workshop on nonlinear signal and image processing, 1995, pp. 254–257.

[19] P. Wellner, *Adaptive thresholding for the digital desk*, Xerox, EPC1993-110, 1993.

[20] A. P. Witkin, *Scale-space filtering: a new approach to multi-scale description*, IEEE International Conference on Acoustics, Speech, and Signal Processing, 1984, pp. 150–153.

Proceedings of the 8th International Symposium on Mathematical Morphology,
Rio de Janeiro, Brazil, Oct. 10–13, 2007, MCT/INPE, v. 1, p. 101–112.
http://urlib.net/dpi.inpe.br/ismm@80/2007/03.19.15.04

Appendix: Proof of the propositions

Proposition 2. First, we prove that the operator defined in Equation 3 performs a dilation on image maximum, that is, $(f \oslash g_\sigma)(\mathbf{x}_{max}) = (f \oplus g_\sigma)(\mathbf{x}_{max})$. To avoid level-shifting and horizontal translation effects, we require that $\sup_{\mathbf{t}\in\mathcal{G}}\{g(\mathbf{t})\} = 0$, and $g(\mathbf{0}) = 0$. Assume that the sup occurs for $t = \zeta$.

$$\begin{aligned}(f \oplus g_\sigma)(\mathbf{x}_{max}) &= \sup_{\mathbf{t}\in\mathcal{N}}\{f(\mathbf{x}_{max} - \mathbf{t}) + g_\sigma(\mathbf{t})\}\\ &= f(\mathbf{x}_{max} - \zeta) + g_\sigma(\zeta)\\ &\leq f(\mathbf{x}_{max} - \zeta) \leq f(\mathbf{x}_{max}).\end{aligned}$$

Since at $\mathbf{t} = \mathbf{0}$ we have $f(\mathbf{x}_{max}) + g_\sigma(\mathbf{0}) = f(\mathbf{x}_{max})$, it follows that $\sup_{\mathbf{t}\in\mathcal{N}}\{f(\mathbf{x}_{max} - \mathbf{t}) + g_\sigma(\mathbf{t})\} = f(\mathbf{x}_{max})$. The proof for $(f \oslash g_\sigma)(\mathbf{x}_{min}) = (f \ominus g_\sigma)(\mathbf{x}_{min})$ is analogous. Based on this, the final proof of Proposition 2 can be found in [4], as well as the proof of Theorem 1.

Proposition 3. The operator defined in Equation 3 can be easily rewritten as

$$(f \oslash g_\sigma)(\mathbf{x}) = \begin{cases} \psi_1^k(\mathbf{x}) & \text{if } f(\mathbf{x}) > \frac{1}{2}(\beta_n + \alpha_n),\\ f(\mathbf{x}) & \text{if } f(\mathbf{x}) = \frac{1}{2}(\beta_n + \alpha_n),\\ \psi_2^k(\mathbf{x}) & \text{otherwise,}\end{cases}$$

with $\alpha_n = \max_{\mathbf{t}\in N(\mathbf{x},k),\mathbf{t}\neq 0}\{f(\mathbf{x}), f(\mathbf{x}-\mathbf{t}) + (-|\sigma_n|^{-1}))\}$ and $\beta_n = \min_{\mathbf{t}\in N(\mathbf{x},k),\mathbf{t}\neq 0}\{f(\mathbf{x}), f(\mathbf{x}-\mathbf{t}) - (-|\sigma_n|^{-1})\}$, where σ_n is the n-th scale and $N(\mathbf{x}, \epsilon)$ represents the set of pixels located in a chess distance less or equal ϵ from $\mathbf{x}$. The sequence (α_n) satisfies:

- $\alpha_n \geq f(\mathbf{x})$;
- (α_n) is monotonically decreasing, i.e., $\alpha_n \geq \alpha_{n+1} \forall n$;
- (α_n) is stationary, i.e., $\exists n_0 / \forall n \geq n_0, \alpha_n = f(\mathbf{x}_0)$.

The sequence (β_k) satisfies:

- $\beta_n \leq f(\mathbf{x})$;
- (β_n) is monotonically increasing, i.e., $\beta_n \leq \beta_{n+1} \forall n$;
- (β_n) is stationary, i.e., $\exists n_0 / \forall n \geq n_0, \beta_n = f(\mathbf{x}_0)$.

Let $\gamma_n = \frac{1}{2}(\alpha_n + \beta_n)$. Since the sequences (α_n) and (β_n) are stationary and monotone, we have that the sequence (γ_n) is both monotonic and stationary [10]. This yields a sequence γ_k that is monotonically increasing or decreasing and converges to the original image value after a certain number of iterations.